Available online at www.sciencedirect.com

SciVerse ScienceDirect

Ceramics International 39 (2013) 4975–4983

CERAMICS INTERNATIONAL

www.elsevier.com/locate/ceramint

Cytocompatibility, bioactivity and mechanical strength of calcium phosphate cement reinforced with multi-walled carbon nanotubes and bovine serum albumin

Fatemeh Gholami[a], Sharif Hussein Sharif Zein[a,*], Lutz-Christian Gerhardt[b,1], Kah Ling Low[a], Soon Huat Tan[a], David S. McPhail[b], Liam M. Grover[c], Aldo R. Boccaccini[b,d]

[a]*School of Chemical Engineering, Engineering Campus, Universiti Sains Malaysia, Seri Ampangan, 14300 Nibong Tebal, SeberangPerai Selatan, Pulau Pinang, Malaysia*

[b]*Department of Materials, Imperial College London, Prince Consort Road, London SW7 2AZ, UK*

[c]*Chemical Engineering, The University of Birmingham, Edgbaston, Birmingham B15 2TT, UK*

[d]*Institute of Biomaterials, Department of Materials Science and Engineering, University of Erlangen-Nuremberg, 91058 Erlangen, Germany*

Received 28 September 2012; received in revised form 27 November 2012; accepted 28 November 2012
Available online 25 December 2012

Abstract

This paper reports on the *in vitro* cytotoxicity, bioactivity behaviour and mechanical properties of novel injectable calcium phosphate cement filled with hydroxylated multi-walled carbon nanotubes and bovine serum albumin (CPC/MWCNT-OH/BSA). To predict the *in vitro* bioactivity of the calcium phosphate composites, we investigated apatite formation on CPC/MWCNT-OH/BSA composites after soaking in simulated body fluid (SBF) for up to 28 days. Compressive strength tests, scanning electron microscopy (SEM), Fourier transform infrared spectroscopy (FTIR), X-ray diffraction (XRD) and cell culture experiments with human CCD-18Co fibroblasts cell lines were performed to evaluate the effect of SBF pre-treatment on the mechanical, structural and biological properties of the CPC/MWCNT-OH/BSA composites. Although apatite formation increased significantly with SBF immersion period, the results showed that all soaked CPC/MWCNT-OH/BSA composites exhibited up to 2.5 times lower compressive strength (13–20 MPa), which were however higher than values reported for the strength of trabecular bone (2–12 MPa). Cell culture experiments showed that low concentrations (6.25 and 12.5 μg/ml) of bio-mineralised CPC/MWCNT-OH/BSA composites led to cell proliferative rather than cytotoxic effects on fibroblasts, evidenced by high cell viabilities (104–113%). The novel CPC/MWCNT-OH/BSA composites presented in this study showed favourable cytocompatible and bioactive behaviour along with high compressive strength (13–32 MPa) and are therefore considered as an attractive bone filling material.

Keywords: Cytotoxicity; *In vitro* bioactivity; Compressive strength; CPCs

1. Introduction

Due to their similarity to the mineral phase of bone, and their *in situ* setting ability, calcium phosphate cements (CPCs) are considered as promising materials to repair bone defects [1]. CPCs have been developed as injectable bone substitutes (IBS) due to their bioactivity, self-setting characteristics, low setting temperature, adequate stiffness and easy shaping into complicated geometries [2,3].

There are currently a number of CPC products commercially available, however they have limited compressive strength. Therefore, the use of CPCs is restricted primarily to non-stress-bearing applications, such as in maxillofacial surgery, the repair of cranial defects and dental fillings [4–6]. Novel CPCs with high mechanical strength, enhanced bioactivity and resorbability must therefore be developed to broaden the application potential of CPCs to restore bone fractures and bone diseases at high load-bearing anatomical sites [7]. To overcome these problems

*Corresponding author. Tel.: +604 599 6442; fax: +604 594 1013.
E-mail address: chhussein@eng.usm.my (S.H.S. Zein).
[1]Present address: Philips Research, Materials Technology, Eindhoven, The Netherlands.

0272-8842/$ - see front matter © 2012 Elsevier Ltd and Techna Group S.r.l. All rights reserved.
http://dx.doi.org/10.1016/j.ceramint.2012.11.094

and challenges, the combination of calcium phosphate with carbon nanotubes (CNTs) is being investigated to exploit the extraordinary mechanical properties of CNTs to reinforce bioceramic matrices [8,9]. CNTs have an excellent potential to reinforce CPCs based on their small dimensions, high aspect ratio (length to diameter) and high strength and stiffness [10]. The addition of CNTs to CPCs is thus expected to improve the mechanical properties of the intrinsically weak CPCs, especially the fracture strength and toughness [7]. To achieve an adequate mechanical reinforcement, the surface of the CNTs must be functionalised to improve the dispersion of individual CNTs in the ceramic matrix and induce an ideal interfacial bonding between the CNTs and the CPCs that could be ultimately responsible for an efficient load-transfer mechanism [9,10]. In the case of CNT-based biomaterials, possible nanotoxicity issues must be considered [11–13], this being one of the key objectives of this paper.

In this paper, we report the *in vitro* cytotoxicity and bioactivity behaviour of bio-mineralised (*i.e.*, pre-treated with SBF), CPC composites incorporated with hydroxylated multi-walled carbon nanotubes (MWCNT-OH) and bovine serum albumin (BSA). The specific objectives were to investigate the influence of the SBF pre-treatment on (a) the bone bonding ability (apatite formation), (b) the mechanical properties of the CPC/MWCNT-OH/BSA composites, and (c) the cytotoxicity of the SBF treated CPC composites (samples were immersed in SBF for 7, 14, 21 and 28 days).

2. Materials and methods

2.1. Sample preparation

The CPC/MWCNT-OH/BSA composites were prepared according to the procedure reported in our previously published paper [14]. Briefly, equimolar fractions of β-tricalcium phosphate, (β-$Ca_3(PO_4)_2$, (β-TCP)) and dicalcium phosphate anhydrous, $CaHPO_4$, (DCPA) were mixed with de-ionised water, 0.5 wt% of hydroxylated MWCNT (MWCNT-OH) and 15 wt% of BSA to produce the CPC/MWCNT-OH/BSA composite. Specifications of the raw materials used and details of the preparation conditions are summarised in Table 1. The CPC starting materials were blended using a mechanical overhead stirrer until a homogeneous paste was obtained. The paste was then firmly packed into a cylindrical stainless steel mould (diameter = 6 mm, height = 12 mm) using a spatula. The packed stainless steel mould was wrapped with a water-soaked wipe to prevent the sample from drying out and then stored in an incubator at 37 °C and 97% humidity for 24 h until further experiments with the samples were performed. Immediately before testing, the samples were taken out and dried at room temperature (24–26 °C).

2.2. Bioactivity experiments

In vitro bioactivity experiments were carried out using simulated body fluid (SBF). SBF, which contains inorganic salt ions nearly equal to those of human blood plasma, was prepared following the procedure proposed by Kokubo and colleagues [15,16]. SBF was prepared by dissolving appropriate amounts of sodium chloride (NaCl), sodium hydrogen carbonate ($NaHCO_3$), potassium chloride (KCl), potassium hydrogenphosphate trihydrate ($K_2HPO_4 \cdot 3H_2O$), magnesium chloride hexahydrate ($MgCl_2 \cdot 6H_2O$), calcium chloride ($CaCl_2 \cdot 2H_2O$) and sodium sulphate (Na_2SO_4) in ultra-pure water, in the order given in Table 2. Chemicals were added one by one after each reagent was completely dissolved. The SBF solution was buffered with 75 mM Tris (hydroxyl-methyl) aminomethane and adjusted at 37 °C to a physiological pH of 7.25 with approximately 67.5 mM hydrochloric acid (HCl).

For bioactivity testing, CPC/MWCNT-OH/BSA composites were immersed in SBF for 0, 7, 14, 21 and 28 days, and incubated at 37 °C under static conditions. At the end of different immersion periods, samples were withdrawn from

Table 2
Reagents for preparation of SBF (pH 7.25, 1 L).

Order	Reagent	Amount
1	NaCl	7.996 g
2	$NaHCO_3$	0.350 g
3	KCl	0.224 g
4	$K_2HPO_4 \cdot 3H_2O$	0.228 g
5	$MgCl_2 \cdot 6H_2O$	0.305 g
6	1 kmol/m^3 HCl	40 cm^3
7	$CaCl_2$	0.278 g
8	Na_2SO_4	0.071 g
9	$(CH_2OH)_3CNH_2$	6.057 g
10	1 kmol/m^3 HCl	Appropriate amount for adjusting pH

Table 1
Specifications of starting materials for CPC/MWCNT-OH/BSA composites.

Raw materials	Size	Supplier
β-TCP	Diameter: 17.30 μm	Sigma-Aldrich
DCPA	Diameter: 11.50 μm	Sigma-Aldrich
MWCNT-OH	Diameter: 30–50 nm, length: ≈ 30 μm	Chinese Academy of Science
BSA	–	Fluka

All experiments were performed under controlled conditions at an ambient temperature of 24–26 °C and at a relative humidity of 50–60%.

SBF, gently washed with de-ionised water and dried at room temperature for 24 h.

2.3. Sample characterisation

2.3.1. Scanning electron microscopy (SEM)

SEM analysis was performed using a Leo Supra 35VP-24-58 microscope to investigate the microstructure and morphology of the composites. Sample fracture fragments were mounted on conducting carbon tape and analysed using an accelerating voltage of 5 kV and a secondary electron detector.

2.3.2. Fourier transform infrared spectroscopy (FTIR)

FTIR spectroscopy was conducted using a Perkin–Elmer FTIR 2000 spectrometer to characterise the presence of specific surface functional groups in the composites. The FTIR spectra were recorded in the wave number interval 400–4000 cm^{-1} using the transmittance mode. Because possible incomplete mixing of the starting materials could have led to heterogeneous apatite formation, 10 different locations of the CPC sample were scanned and averaged. The resolution of the spectrometer was 4 cm^{-1}. Before analysis, calibration of the spectrometer was performed with polystyrene as a control sample. The test sample was mixed with potassium bromide using a weight ratio of approximately 1:10. The mixture was ground to a fine, homogeneous powder which was then poured into a mould. The powder was compacted using a hydraulic press by applying a pressure of $\approx$600 MPa to form thin pellets (thickness of $\approx$100 μm). The resulting pellet was then placed in the sample holder for FTIR analyses.

2.3.3. X-ray diffraction (XRD) analysis

A Siemens D-5000 X-ray diffractometer was used to identify the chemical composition of the crystalline phases in the CPC/MWCNT-OH/BSA composites before and after immersion in SBF. XRD patterns were recorded over a 2θ angle range of 25–65° at a sweep rate of 0.04° s^{-1}. The crystallinity of the different materials investigated was qualitatively assessed by comparing the characteristic element-specific peaks of the XRD pattern from the CPC samples with standard diffraction patterns of specific compounds based on the International Centre for Diffraction Data (ICDD).

2.3.4. Mechanical testing

The compressive strength of the cylindrical specimens (diameter = 6 mm, height = 12 mm) was tested using an Instron 3367 universal testing machine at a crosshead speed of 1.0 mm/min. Before mechanical testing, samples were dried and the bottom and top sides of samples were filed flushed to ensure that the test specimens had plane-parallel surfaces to avoid shear failure during testing. The compressive engineering strength was determined on the basis of maximum compressive force and the nominal cross-sectional area of the scaffolds. Two samples of each scaffold composition were investigated.

2.4. Cytotoxicity testing

The cytotoxicity of the composites was assessed using human fibroblasts cells (CCD-18Co), which were inoculated and exposed to different concentrations of CPC/MWCNT/BSA powder (0–200 μg/ml) obtained through grinding the particle mixture of starting materials (Table 2).

2.4.1. Maintenance of cell culture

CCD-18Co cells were cultured in Dulbecco's Modified Eagle's Medium (DMEM, Invitrogen Life Technologies, Karlsruhe, Germany) supplemented with 10% foetal bovine serum; the cells were incubated in a humidified 5% CO_2 incubator at 37 °C.

2.4.2. Cell seeding and treatment of cells with CPC/MWCT/BSA powder

Prior to inoculation with CPC/MWCNT/BSA particles, the fibroblasts were seeded in 96-well plates with a density of 1.5×10^5 cells per well and allowed to attach for 12 h before further treatment. The ground CPC/MWCNT/BSA powder was diluted with cell culture medium to obtain the desired concentrations of 6.25, 12.5, 25, 50, 100 and 200 μg/ml. Into each well containing the cells, 100 μL of fresh medium supplemented with CPC/MWCNT/BSA particle concentrations between 6.25 μg/ml and 200 μg/ml was added. To the control wells (*i.e.*, untreated cells), only 100 μl of cell culture medium (no particles) was added.

2.4.3. MTT viability assay

The mitochondrial respiratory activity of the fibroblasts treated with CPC/MWCNT/BSA composite particles was determined colourimetrically using MTT ((3-(4,5-dimethylthiazol-2-yl)-2,5-diphenyltetrazolium bromide) assays, as previously reported [17]. MTT salt solution (5 mg/ml) was added 4 h prior to the end of the 72 h sample incubation to allow cellular tetrazolium metabolism. After 4 h, cell culture medium and MTT solution was aspirated, and the MTT lysis solution (DMSO) was added into the wells to solubilise formazan crystals, and the plates were incubated for 5 min before absorption was read at a wavelength of 570 nm with a reference wavelength of 620 nm (ELISA microplate reader, Ascent Multiskan). For each analysis, the samples were examined in triplicates, and the average and standard deviation were calculated. Results were reported as percentage of cell viability and expressed as the mean ± standard deviation. The percentage of viable cells was calculated from the optical density (O.D.) values using Eqs. (1) and (2) respectively:

$$\%\ \text{Cell Inhibition} = \frac{\text{O.D. value (control cells)} - \text{O.D. value (treated cells)}}{\text{O.D. value (control cells)}} \times 100 \quad (1)$$

$$\%\ \text{Cell viability} = 100 - \%\ \text{Cell Inhibition} \quad (2)$$

2.5. Statistics

Statistical analyses were conducted with SPSS (version 17.0). Group means and standard deviations (SD) were calculated for the compressive strength test at different immersion times (0, 7, 14, 21 and 28 days) and for the cell viability tests at different concentrations of CPC/MWCNT-OH/BSA composites (6.25, 12, 25, 50, 100 and 200 μg/ml). Statistical analysis was performed by one-way ANOVA and Tukey's test and the statistical significance was considered at probability values of $p < 0.05$.

3. Results and discussion

3.1. In vitro bioactivity of CPC composites: microstructural analysis

3.1.1. Scanning electron microscopy

The formation of apatite was verified by SEM observations (Fig. 1), FTIR and XRD analyses. Fig. 1(a–e) shows the SEM micrographs of the HA crystals and the HA layer structural features of the CPC/MWCNT-OH/BSA composites for the unsoaked samples and the samples soaked in SBF for 7, 14, 21 and 28 days. Fig. 1(a) shows that in the unsoaked CPC/MWCNT-OH/BSA composite, fine and well-packed apatite crystals are relatively homogeneously distributed on the surface of the cement. However, upon immersion in SBF, there is a rougher and more irregularly shaped apatite layer on the CPC/MWCNT-OH/BSA composites (Fig. 1(b–e)). The formation of crystals with morphology like apatite were observed on the surface of the CPC/MWCNT-OH/BSA composite after 7 days (Fig. 1(b)), whereas rough and irregular rigid shapes of bone-like apatite layers were formed after 14 days of soaking in SBF (Fig. 1(c)). Upon immersion in SBF for 21 days, one can observe that apatite crystal agglomerates of a rigid cube shape were developed, as shown in Fig. 1(d). Fig. 1(e) shows an apatite layer that possess a subtle net-like texture link with MWCNT-OH for the CPC/MWCNT-OH/BSA composite soaked in SBF for 28 days. The different morphologies of HA formation discussed above were also found in studies by Aryal et al. [18], Li et al. [19] and Boccaccini et al. [20].

In this study, the immersion in SBF has triggered/induced the formation of an apatite layer on the surface of the CPC/MWCNT-OH/BSA composites. Traditionally, the *in vitro* bioactivity of the materials has been evaluated by their incubation in SBF over various time periods and by studying the possible formation of apatite and bone bonding ability [21–26], although there is an ongoing scientific debate on the significance of results obtained from immersion into protein-lacking SBF [6,27]. Nevertheless, *in vitro* investigations using SBF are considered useful for gaining insight and knowledge on the physical chemistry of bio-mineralisation. Drawing on the results of our SEM micrographs, as well as FTIR and XRD analyses (see below), the phenomenon of apatite nucleation demonstrated the bioactive properties of the CPC/MWCNT-OH/BSA composites studied here. In addition, the apatite layers formed are considered to be chemically stable due to their chemical similarity to the CPC starting materials; thus, the developed CPC is expected to enhance bone bonding at the composite interface because a bone-like apatite layer is playing a crucial role in establishing the bone bonding interface between biomaterials and living tissue [28]. In addition to the bone bonding ability, the nano-topographical features provided by the incorporation of CNTs into the CPC matrix might improve bone formation. Nano-scale surface topography has normally been associated with increased cellular functions, higher protein adsorption, cell proliferation and differentiation [29,30].

3.1.2. Fourier transform infrared (FTIR) spectroscopy

The FTIR spectra of the CPC/MWCNT-OH/BSA composites immersed in SBF for 0, 7, 14, 21 and 28 days are summarised in Fig. 2(a–e) respectively. FTIR spectroscopy confirmed the observations made on the SEM images discussed above and provided evidence of the formation of an appetite layer on the different CPCs studied. The absorption bands at 3297–3307 cm^{-1} and 3400–3500 cm^{-1} corresponded to the strong characteristic peak of the stretching mode of the hydroxyl group (–OH) [31–33]. Subsequently, the sputtering target was comprised primarily of crystalline HA. From Fig. 2(a–e), the peaks pertaining to the HA phase were the hydroxyl bands at 3298 cm^{-1}, 3409 cm^{-1} and 3411 cm^{-1}, and this sputtering target was comprised primarily of the crystalline HA.

By comparing the results of the different FTIR spectra, it was found that the absorption bands for the CPC/MWCNT-OH/BSA composite immersed in SBF for 28 days (Fig. 2(e)) gave the appearance of several sharper –OH bands at 3409 cm^{-1}, P–O bands (ν_1 mode) at 965 cm^{-1} [34,35], P–O bands (ν_3 mode) at 1121 cm^{-1} and P–O bands (ν_4 mode) at 604 cm^{-1} and 551 cm^{-1} [36]. This finding may indicate that crystalline apatite was formed in the CPC/MWCNT-OH/BSA composite immersed in SBF for 28 days.

3.1.3. X-ray diffraction analysis

Fig. 3(a–e) shows the XRD patterns of the CPC/MWCNT-OH/BSA composites obtained upon soaking in SBF for 0, 7, 14, 21 and 28 days. Diffraction peaks corresponding to the HA crystalline phase were found at 2θ angles of 26°, 29°, 32°, 40° and 53°. The presence of an intense diffraction peak at the 2θ angle of 26° revealed the growth of the apatite crystal along the *c*-axis [37]. The XRD results support the conclusion that apatite was formed on the CPC, which is correlated with the crystal morphology observed by SEM [32,38–40] (Fig. 3(c–e)). However, as seen in Fig. 3, the XRD analysis also revealed two extra phases of the starting materials corresponding to β-TCP and DCPA, indicating that the reaction to form HA was not complete. In conclusion, SEM, FTIR and

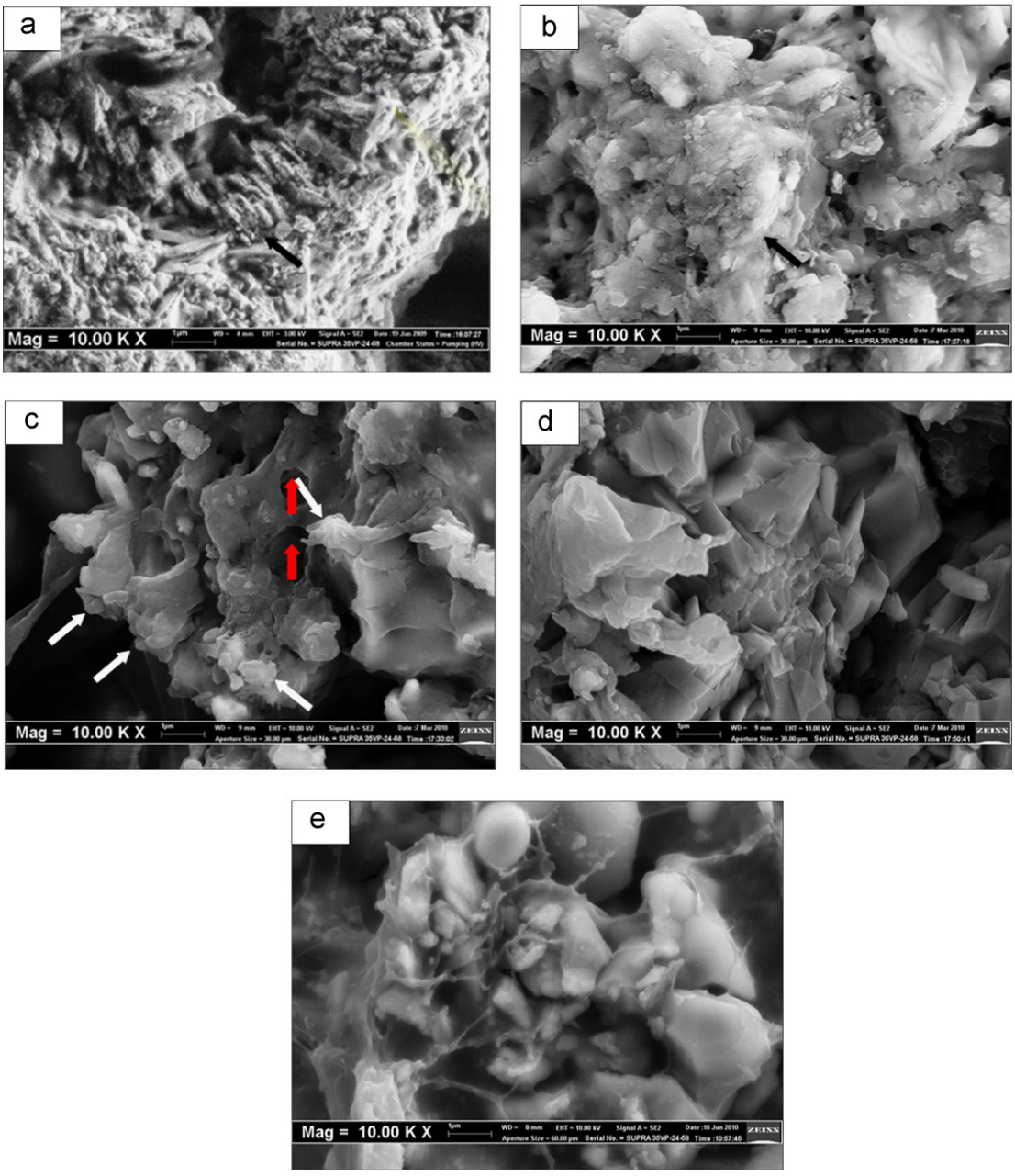

Fig. 1. SEM micrographs of CPC/MWCNT-OH/BSA composites following immersion in SBF for (a) unsoaked, (b) 7 days, (c) 14 days, (d) 21 days and (e) 28 days (arrows indicate different forms of apatite, discussed in Sections 3.1.1 and 3.2). (For interpretation of the references to color in this figure legend, the reader is referred to the web version of this article.)

XRD results showed that the herein investigated CPC/MWCNT-OH/BSA composites developed a crystalline apatite phase that is similar to the mineral phase of bone in its chemical and crystallographic composition [41].

3.2. Mechanical properties—compressive strength

Fig. 4 shows the compressive strength of CPC/MWCNT-OH/BSA composites after immersion in SBF for 0, 7, 14, 21 and 28 days. Compared with the unsoaked CPC/MWCNT-OH/BSA composites (31.94 MPa), the compressive strength of the CPC/MWCNT-OH/BSA composites decreased significantly with immersion duration in SBF. For a similar CPC matrix and CNT loading, Wang et al. [42] found for 0.5 wt% bio-mineralised CNT/CPC composites compressive strength values of 55 MPa.

In this study, we used the bio-mineralisation process to study the effect of SBF pre-treatment of the CPC/MWCNT-OH/BSA composite on compressive strength rather than that (effect) arising from surface functionalisation of individual CNTs [40,42]. The effect of CNT surface functionalisation on the mechanical properties for CPC/BSA composites containing 0.5 wt% MWCNT-OH has been presented in a previous paper of our group [43]. Briefly, the MWCNTs-OH was soaked in SBF for 7 days to synthesize bio-mineralized MWCNTs-OH. The

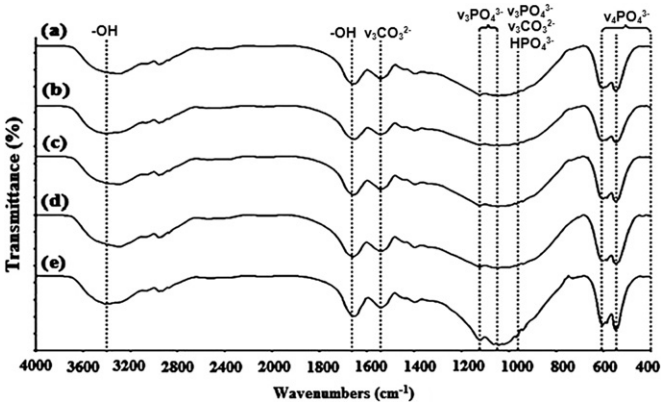

Fig. 2. FTIR patterns of CPC/MWCNT-OH/BSA composites following immersion in SBF for (a) unsoaked, (b) 7 days, (c) 14 days, (d) 21 days and (e) 28 days.

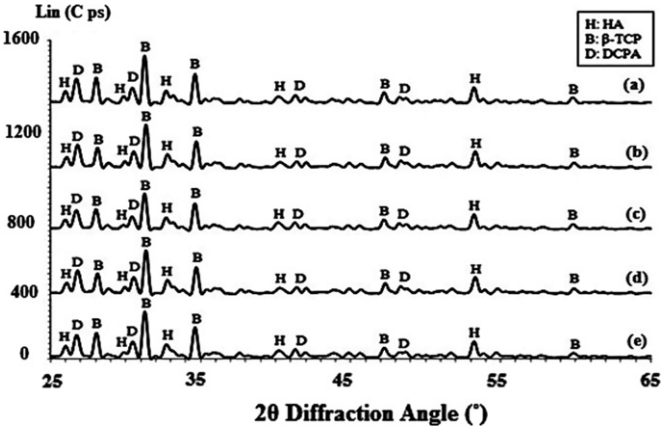

Fig. 3. X-ray diffraction patterns of CPC/MWCNT-OH/BSA composites following immersion in SBF for (a) unsoaked, (b) 7 days, (c) 14 days, (d) 21 days and (e) 28 days.

bio-mineralized MWCNTs-OH was mixed with CPC and BSA to obtain the composites. The results indicated that the strong interfacial bonding of CPC/MWCNTs-OH is essential to improve the mechanical properties of CPC/bio-mineralized MWCNTs-OH/BSA composite.

As shown in Fig. 4, there was a significant reduction in the compressive strength of the CPC/MWCNT-OH/BSA composites that were immersed in SBF for 7, 14, 21 and 28 days ($p < 0.05$) compared to unsoaked CPC/MWCNT-OH/BSA composites, indicating the continuous and slow formation of bone-like apatite layers on the surface of the cement (see SEM images and XRD). However, the SEM images showed that after immersion in SBF, degradation of CPC may increase the porosity of the composite (the red arrows in Fig. 1(c) shows the degradation holes), thus the composite may collapse more easily due to the decreased compressive strength.

3.3. Cytotoxicity

The cytotoxicity of the new CPC/MWCNT/BSA composites was evaluated in terms of mitochondrial

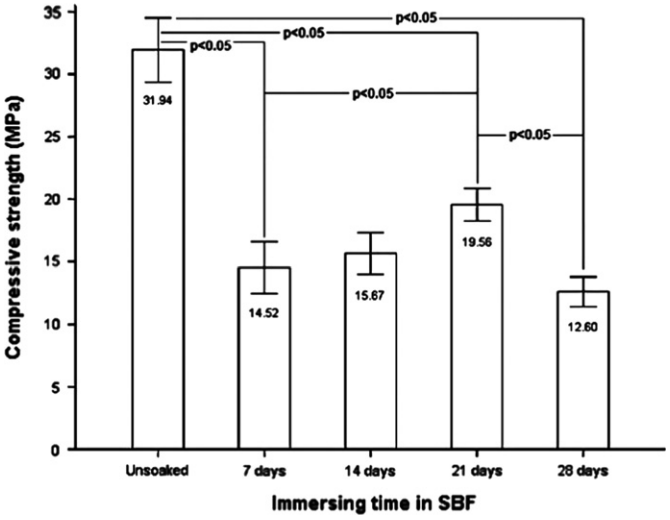

Fig. 4. Compressive strength of CPC/MWCNT-OH/BSA composites following immersion in SBF for unsoaked, 7, 14, 21 and 28 days. Data are presented as the means ± 2 standard deviation ($n = 2$).

respiratory activity of human fibroblasts. The influence of CPC/MWCNT-OH/BSA composites on CCD-18Co fibroblast metabolic activity is shown in Fig. 5. There was a significant reduction in the viability of CCD-18Co human fibroblast cells with increasing CPC-MWCNT particle concentration from 6.25 μg/ml to 200 μg/ml ($p < 0.001$)
at 7, 14, 21 and 28 days of immersion. For each SBF immersion time point, MTT assays revealed significantly decreasing human fibroblast cell viability with increasing CPC composite powder concentration. Low concentrations of the CPC/MWCNT-OH/BSA composite (6.25, 12.5 μg/ml) did not adversely affect human fibroblast cell viabilities at all time points studied. Here, it is interesting to note that at the lowest concentration (6.25 μg/ml), there was a tendency towards higher cell viabilities (102–133%; Fig. 5), indicating a cell proliferative effect of the CPC/MWCNT-OH/BSA composite as evidenced by a higher metabolic activity of the fibroblasts. Despite the promising results found for low concentrations of CPC-MWCNT-BSA particles, the impaired cell viabilities (60–70%) for higher concentrations (100–200 μg/ml) indicate slight cytotoxic effects. Thus, uncontrolled release of particles or wearing of the CPC-composite at the implantation site should be avoided.

Previous workers studied the toxicity of carbon nanotubes using cell lines [44,45] or animal models [46–48]. The results of these studies are contradictory; some of them indicate that CNTs are highly toxic [44] whereas others showed non-toxic effects [45,47]. For example, Cui et al. studied the treatment of the human embryonic kidney (HEK) 293 cells with single-walled CNTs (SWCNTs). Their result showed a time and dose dependent reduction in cell viability [44]. Another experiment that was conducted on human promyelocytic leukaemia (HL) cells (HL-60) demonstrated that SWCNTs up to 25 μg/mL do

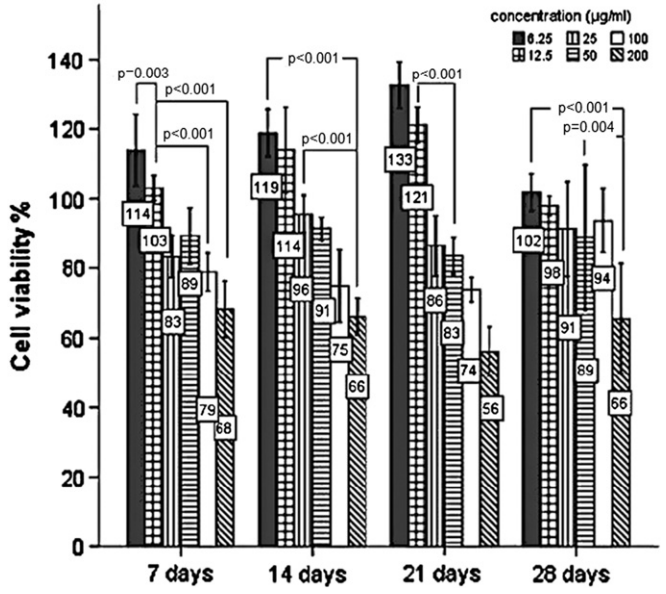

Fig. 5. Influence of CPC/MWCNT-OH/BSA composites on CCD-18Co fibroblast metabolic activity as measured using MTT assay (data are presented as the means ± 2 standard deviations, $n = 3$).

not have a proliferative effect on cells or on the viability of the cells if the cells are exposed to CNTs for a short time (for example, 2 h) [49]. Muller et al. studied the *in vitro* and *in vivo* effects of MWCNTs on epithelial cells and showed the possibility of adverse effects of the MWCNTs [50].

Due to the above-mentioned obscurities with regard to the cytotoxicity of carbon nanotubes [11–13], there are clearly more extended *in vivo* and *in vitro* studies necessary before clinical applications can be realised and the product can be commercialised for tissue engineering and biomedical products.

3.4. CPC composites as bone substitutes

We used β-TCP and DCPA as the main components of the CPC material because this particular combination allows control over the degradation and bioactivity behaviour of the CPC to promote bone formation, as stated by Kitamura et al. [51]. The as-prepared CPC material presented here is capable of self-setting at 37 °C (normal body temperature, setting time approximately 30 min) and is thus useful for bone substitutes, as shown in our previous study on CPC [14].

The mixtures of β-TCP and DCPA for bone substitution have been used for many years [52], and β-TCP has been reported a promising merit in bone formation as a candidate material for bone graft [53]. By adding β-TCP, the overall resorption rate of the cement can be tailored to specific needs, and bone formation rate can be controlled. For example, cements containing β-TCP and DCPA have been found to completely degrade in 16 weeks *in vivo* [52]. In this study, the CPC was mixed with MWCNT-OH and incorporated with BSA to form CPC/MWCNT-OH/BSA composites. In accordance with our previous study [14], BSA was found to act as a promoter of HA growth when bound to the surface of CPC grains (see also FTIR and SEM results, as discussed above). We suggested in our previous paper [14] that admixture of MWCNT-OH improves the interfacial bonding between the filler and the CPC matrix, leading to a higher compressive strength than MWCNT-COOH-containing CPC. In this study, the diminished enhancing effect of MWCNT-COOH is due to the impaired capability of attracting both Ca^{2+} and PO_4^{3-} ions for nucleating and growing HA crystals. CPC/MWCNT-OH/BSA composites were therefore selected in this study to investigate their *in vitro* safety profile and biological effect.

4. Conclusions

In this study, CPC/MWCNT-OH/BSA composites were immersed in SBF for various periods of time (0, 7, 14, 21 and 28 days). The results showed that unsoaked CPC/MWCNT-OH/BSA composites had the highest compressive strength (32 MPa) and a high bioactive behaviour through a continuous formation of apatite. SEM and FTIR results showed that highly crystalline apatite was formed in the CPC/MWCNT-OH/BSA composites following immersion in SBF for 28 days. Cell culture experiments showed that low concentrations of bio-mineralised CPC/MWCNT-OH/BSA composites led to cell proliferative rather cytotoxic effects to fibroblasts, demonstrated by high cell viabilities.

The novel CPC/MWCNT-OH/BSA composites presented in this study showed favourable cytocompatible and bioactive behaviour along with relatively high compressive strength (32 MPa) and they can be therefore considered an attractive bone filling material.

Acknowledgements

The work was financially supported by the British Council through the UK's Prime Minister's Initiative for International Education (PMI2) Connect scheme and USM-RU grant.

References

[1] H.P. Yuan, Y.B. Li, J.D. Bruijn, K. Groot, X.D. Zhang, Tissue responses of calcium phosphate cement: a study in dogs, Biomaterials 21 (2000) 1283–1290.
[2] X.P. Wang, J.D. Ye, Y.J. Wang, L. Chen, Self-setting properties of a b-dicalcium silicate-reinforced calcium phosphate cement, Journal of Biomedical Materials Research Part B: Applied Biomaterials 82 (1) (2007) 93–99.
[3] E. Fernandez, Bioactive bone cements, in: Metin Akay (Ed.), Wiley Encyclopedia of Biomedical Engineering, John Wiley & Sons, Inc., NY, 2006, pp. 1–9.
[4] C.D. Friedman, P.D. Costantino, S. Takagi, L.C. Chow, BoneSourceTM hydroxyapatite cement: a novel biomaterial for craniofacial skeletal tissue engineering and reconstruction, Journal of

Biomedical Materials Research Part B: Applied Biomaterials 43 (1998) 428–432.
[5] J.P. Schmitz, J.O. Hollinger, S.B. Milam, Reconstruction of bone using calcium phosphate bone cements: a critical review, Journal of Oral and Maxillofacial Surgery 57 (1999) 1122–1126.
[6] M. Bohner, J. Lemaitre, Can bioactivity be tested *in vitro* with SBF solution?, Biomaterials 30 (12) (2009) 2175–2179
[7] K.L. Low, S.H. Tan, S.H.S. Zein, J.A. Roether, V. Mouriño, A.R. Boccaccini, Review: calcium phosphate-based composites as injectable bone substitute materials, Journal of Biomedical Materials Research Part B: Applied Biomaterials 94B (2010) 273–286.
[8] A.R. Boccaccini, L.C. Gerhardt, Carbon nanotube composite scaffolds and coatings for tissue engineering applications, Key Engineering Materials: Advanced Bioceramics in Nanomedicine and Tissue Engineering 441 (2010) 31–52.
[9] A.R. Boccaccini, J. Cho, T. Subhani, C. Kaya, F. Kaya, Electrophoretic deposition of carbon nanotube–ceramic nanocomposites, Journal of the European Ceramic Society 30 (2010) 1115–1129.
[10] A.A. White, S.M. Best, I.A. Kinloch, Hydroxyapatite–carbon nanotube composites for biomedical applications: a review, International Journal of Applied Ceramic Technology 4 (1) (2007) 1–13.
[11] K. Aschberger, H.J. Johnston, V. Stone, R.J. Aitken, C.L. Tran, S.M. Hankin, S.A.K. Peters, F.M. Christensen, Review of fullerene toxicity and exposure—appraisal of a human health risk assessment, based on open literature original research article, Regulatory Toxicology and Pharmacology 58 (3) (2010) 455–473.
[12] P. Diot, J. Pairon, C.J. Boczkowski, M. Guillot-Gautier, N. Glas, Effetsrespiratoires de l'inhalation de nanoparticules original research article, Revue des Maladies Respiratoires Actualités 2 (4) (2010) 365–367.
[13] H.F. Krug, B. Rothen-Rutishauser, P. Wick, A comparison of acute and long-term effects of industrial multiwalled carbon nanotubes on human lung and immune cells *in vitro*, Toxicology Letters 200 (3–5) (2011) 176–186.
[14] K.K. Chew, K.L. Low, S.H.S. Zein, D.S. McPhail, L.C. Gerhardt, J.A. Roether, A.R. Boccaccini, Reinforcement of calcium phosphate cement with multi-walled carbon nanotubes and bovine serum albumin for injectable bone substitute applications, Journal of the Mechanical Behavior of Biomedical Materials 4 (3) (2011) 331–339.
[15] T. Kokubo, Bioactive glass ceramics: properties and applications, Biomaterials 12 (1991) 155–163.
[16] O. Chikara, How to prepare the simulated body fluid (SBF) and its related solutions, proposed by Kokubo and his colleagues. Available from: 〈http://mswebs.naist.jp/LABs/tanihara/ohtsuki/SBF/index.html〉 (accessed Jan 2010).
[17] T. Mosmann, Rapid colorimetric assay for cellular growth and survival: application to proliferation and cytotoxicity assays, Journal of Immunological Methods 65 (1–2) (1983) 55–63.
[18] S. Aryal, S.R. Bhattarai, K.C. RemantBahadur, M.S. Khil, D.R. Lee, H.Y. Kim, Carbon nanotubes assisted biomimetic synthesis of hydroxyapatite from simulated body fluid, Materials Science Engineering A 426 (1–2) (2006) 202–207.
[19] H. Liu, H. Li, W.J. Cheng, Y. Yang, M.Y. Zhu, C.R. Zhou, Novel injectable calcium phosphate/chitosan composites for bone substitute materials, Acta Biomaterialia 2 (5) (2006) 557–565.
[20] A.R. Boccaccini, F. Chicatun, J. Cho, O. Bretcanu, J.A. Roether, S. Novak, Q.Z. Chen, Carbon nanotube coatings on bioglass-based tissue engineering scaffolds, Advanced Functional Materials 17 (15) (2007) 2815–2822.
[21] P. Li, C. Ohtsuki, T. Kokubo, K. Nakanishi, N. Soga, T. Nakamura, T. Yamamuro, Process of formation of bone-like apatite layer on silica gel, Journal of Materials Science: Materials in Medicine 4 (1993) 127–131.
[22] T. Kokubo, Apatite formation on surfaces of ceramics, metals and polymers in body environment, Acta Materialia 7 (1998) 2519–2527.
[23] H. Kaneko, M. Uchida, H.M. Kim, T. Kokubo, T. Nakamura, Process of apatite formation induced by anatase on titanium metal in simulated body fluid, Key Engineering Materials 218–220 (2002) 649–652.
[24] P. Siriphannon, Y. Kameshima, A. Yasumori, K. Okada, S. Hayashi, Comparative study of the formation of hydroxyapatite in simulated body fluid under static and flowing system, Journal of Biomedical Materials Research 60 (2002) 175–185.
[25] S. Fujibayashi, M. Neo, H.M. Kim, T. Kokubo, T. Nakamura, A comparative study between *in vivo* bone ingrowth and *in vitro* apatite formation on Na_2O–CaO–SiO_2 glasses, Biomaterials 24 (2003) 1349–1356.
[26] X. Lu, Y. Leng, Theoretical analysis of calcium phosphate precipitation in simulated body fluid, Biomaterials 26 (2005) 1097–1108.
[27] T. Kokubo, H. Takadama, How useful is SBF in predicting *in vivo* bone bio-activity?, Biomaterials 27 (2006) 2907–2915.
[28] L.L. Hench, Bioceramics, from concept to clinic, Journal of the American Ceramic Society 74 (1991) 1482–1510.
[29] L. Zhang, T.J. Webster, Nanotechnology and nanomaterials: promises for improved tissue regeneration, Nano Today 4 (2009) 66–80.
[30] M.S. Lord, M. Foss, F. Besenbacher, Influence of nanoscale surface topography on protein adsorption and cellular response, Nano Today 5 (2010) 66–78.
[31] M.P. Mahabole, R.C. Aiyer, C.V. Ramakrishna, B. Sreedhar, R.S. Khairnar, Synthesis, characterization and gas sensing property of hydroxyapatite ceramic, Bulletin of Material Science 28 (6) (2005) 535–545.
[32] W. Janusz, E. Skwarek, S. Pasieczna-Patkowska, A. Slosarczyk, Z. Paszkiewicz, A. Rapacz-Kmita, A study of surface properties of calcium phosphate by means of photoacoustic spectroscopy (FT-IR/PAS), potentiometric titration and electrophoretic measurements, European Physical Journal Special Topics (2008) 329–333.
[33] S.P. Victor, T.S.S. Kumar, Processing and properties of injectable porous apatitic cements, Journal of the ceramic Society of Japan 116 (2008) 105–107.
[34] A. Slosarczyk, C. Paluszkiewicz, M. Gawlicki, Z. Paszkiewicz, The FTIR spectroscopy and QXRD studies of calcium phosphate based materials produced from the powder precursors with different Ca/P ratios, Ceramic International 23 (8) (1997) 297–304.
[35] E. Park, R.A. Condrate, D. Lee, Infrared spectral investigation of plasma spray coated hydroxyapatite, Materials Letter 36 (1998) 38–43.
[36] Y. Xiao, T. Gong, S. Zhou, The functionalization of multi-walled carbon nanotubes by *in situ* deposition of hydroxyapatite, Biomaterials 31 (19) (2010) 5182–5190.
[37] R. Murugan, S. Ramakrishna, Crystallographic Study of hydroxyapatite bioceramics derived from various sources, Crystal Growth and Design 5 (2005) 111–112.
[38] L.E. Carey, H.H. Xu Jr., C.G. Simon, S. Takagi, L.C. Chow, Premixed rapid-setting calcium phosphate composites for bone repair, Biomaterials 26 (24) (2005) 5002–5014.
[39] H.H.K. Xu, M.D. Weir, C.G. Simon, Injectable and strong nanoapatite scaffolds for cell/growth factor delivery and bone regeneration, Dental Materials 24 (9) (2008) 1212–1222.
[40] X.P. Wang, J.D. Ye, Y.J. Wang, X.P. Wu, B. Bo, Control of crystallinity of hydrated products in a calcium phosphate bone cement, Journal of Biomedical Materials Research Part A 81 (4) (2007) 781–790.
[41] M. Bohner, G. Baroud, Injectability of calcium phosphate pastes, Biomaterials 26 (13) (2005) 1553–1563.
[42] X.P. Wang, J.D. Ye, Y.J. Wang, L. Chen, Reinforcement of calcium phosphate cement by bio-mineralized carbon nanotube, Journal of the American Ceramic Society 90 (3) (2007) 962–964.
[43] K.L. Low, S.H.S. Zein, S.H. Tan, D.S. McPhail, A.R. Boccaccini, The effect of interfacial bonding of calcium phosphate cements containing bio-mineralized multi-walled carbon nanotube and bovine serum albumin on the mechanical properties of calcium phosphate cements, Ceramics International 37 (2011) 2429–2435.
[44] D. Cui, F. Tian, C.S. Ozkan, M. Wang, H. Gao, Effect of single wall carbon nanotubes on human HEK293 cells, Toxicology Letters 155 (1) (2005) 73–85.

[45] H.N. Yehia, R.K. Draper, C. Mikoryak, E.K. Walker, P. Bajaj, I.H. Musselman, M.C. Daigrepont, G.R. Dieckmann, P. Pantano, Single-walled carbon nanotube interactions with HeLa cells, Journal of Nanobiotechnology 5 (2007) 8.

[46] R. Singh, D. Pantarotto, L. Lacerda, G. Pastorin, C. Klumpp, M. Prato, A. Bianco, K. Kostarelos, Tissue biodistribution and blood clearance rates of intravenously administered carbon nanotube radiotracers, Proceedings of the National Academy of Sciences of United States of America 103 (2006) 3357–3362.

[47] T.K. Leeuw, R.M. Reith, R.A. Simonette, M.E. Harden, P. Cherukuri, D.A. Tsyboulski, K.M. Beckingham, R.B. Weisman, Single walled carbon nanotubes in the intact organism: near-IR imaging and biocompatibility studies in Drosophila, Nano Letters 7 (2007) 2650–2654.

[48] Z. Li, T. Hulderman, R. Salmen, R. Chapman, S.S. Leonard, S.H. Young, A. Shvedova, M.I. Luster, P.P. Simeonova, Cardiovascular effects of pulmonary exposure to single-wall carbon nanotubes, Environmental Health Perspectives 115 (2007) 377–382.

[49] N.W. Kam, H. Dai, Carbon nanotubes as intracellular protein transporters: generality and biological functionality, Journal of the American Chemical Society 127 (2005) 6021–6026.

[50] J. Muller, I. Decordier, P.H. Hoet, N. Lombaert, L. Thomassen, F. Huaux, D. Lison, M. Kirsch-Volders, Clastogenic and aneugenic effects of multi-wall carbon nanotubes in epithelial cells, Carcinogenesis 29 (2008) 427–433.

[51] M. Kitamura, C. Ohtsuki, H. Iwasaki, S. Ogata, M. Tanihara, T. Miyazaki, The controlled resorption of porous alpha-tricalcium phosphate using a hydroxypropylcellulose coating, Journal of Materials Science: Materials in Medicine 15 (2004) 1153–1158.

[52] Y. Weitao, K. Kangmei, J. Anmin, An injectable cement: synthesis, physical properties and scaffold for bone repair, Journal of Postgraduate Medicine 53 (2007) 34–38.

[53] N.E. Epstein, A preliminary study of the efficacy of beta tricalcium phosphate as a bone expander for instrumented posterolateral lumbar fusions, Journal of Spinal Disorders and Technique 19 (2006) 424–429.